

Single Cells as Biosensors for Chemical Separations

Jason B. Shear,* Harvey A. Fishman, Nancy L. Allbritton,†
Delia Garigan, Richard N. Zare,‡ Richard H. Scheller

A biosensor system based on the response of living cells was demonstrated that can detect specific components of a complex mixture fractionated by a microcolumn separation technique. This system uses ligand-receptor binding and signal-transduction pathways to biochemically amplify the presence of an analyte after electrophoretic separation. The transduced signal was measured by means of two approaches: (i) fluorescence determination of intracellular calcium concentrations in one or more rat PC-12 cells and (ii) measurement of transmembrane current in a *Xenopus laevis* oocyte microinjected with messenger RNA that encodes a specific receptor. This analysis system has the potential to identify biologically active ligands present in a complex mixture with exceptional sensitivity and selectivity.

Biosensors detect chemical species with high selectivity on the basis of molecular recognition rather than the physical properties of analytes (1). Many types of biosensing devices have been developed in the past 30 years, including enzyme electrodes, optical immunosensors, ligand-receptor amperometers, and evanescent-wave probes (2). Entire living cells also can be used as biosensors (3). Whole-cell biosensors have two important advantages. First, many disparate chemical species can evoke a response from a single cell. Second, the recognition event for a component can be amplified by signal-transduction pathways so that measurable responses result from minute quantities of material (4). When more than one component in a sample mixture elicits a response, however, the signal from a living cell often cannot be interpreted. Consequently, fractionating components before they interact with the cell would be useful. The microcolumn separation technique of capillary electrophoresis (CE) is well suited for this purpose because of its physiologic compatibility (it uses aqueous separation buffers), speed (typically 5- to 30-min analysis times), and high separation efficiency (typically $>10^5$ theoretical plates) (5). In addition, the ability of capillary separations to work with very small samples (picoliter to nanoliter injection volumes) often makes it possible to analyze the components of individual cells

without prohibitive dilution (6). Nevertheless, fractionation of biological samples with many components has proved difficult for CE (7), and a variety of important biological species are not easily detected with traditional measurement approaches (8).

Here, we demonstrate the feasibility of overcoming these limitations by coupling capillary electrophoresis to biosensors that use the responses of single cells. Determination of acetylcholine (ACh) in the lysate of nerve growth factor (NGF)-differentiated rat PC-12 cells illustrates the ability of this approach to rapidly identify chemical species with high specificity. The sensitivity of this technique is shown to be competitive with the best available analysis methods and holds potential for significant improvement.

In two separate single-cell biosensor (SCB) systems for CE, rapid separation of analytes is accomplished in a fused silica capillary, and the effluent from the capillary outlet is directed to an SCB for detection (9). Electroosmosis (bulk solution flow) delivers positive, neutral, and negative species that are separated by CE to the extracellular surface of one or more living cells. The first SCB detector we developed (Fig. 1A) is sensitive to analytes that elicit a change in cytosolic Ca^{2+} concentration ($[Ca^{2+}]_i$) in cultured rat PC-12 cells. Changes in $[Ca^{2+}]_i$ are monitored with fluorescence microscopy with the use of the Ca^{2+} indicator fluo-3 (10). A transmitted-light image taken through the microscope objective (Fig. 2) shows how the outlet of a capillary with an inside diameter (i.d.) of 25 μm can be positioned above a single cell. The second SCB device (Fig. 1B) detects species that cause changes in plasma membrane ion permeability. Two-electrode voltage-clamp measurements were performed on a *Xenopus laevis* oocyte expressing a specific receptor after microinjection of mRNA (11). To

help isolate the electric field used in the CE separation from the small electrical signal measured at the oocyte, we placed the electrophoresis ground upstream from the capillary outlet (12).

The CE-SCB system was able to separate and detect specific components from a mixture (Fig. 3A). A standard solution containing ACh, bradykinin (BK), and adenosine triphosphate (ATP) was separated, and the capillary effluent was delivered to a small group of PC-12 cells. Increases in $[Ca^{2+}]_i$ after ligand-receptor binding are caused by release from internal stores and by entry through ligand- or voltage-gated channels (13). We identified the three peaks in Fig. 3A by electrophoretically separating each component individually (Fig. 3, B, C, and D). Because of the relative charge-to-frictional drag ratios, ACh migrates fastest to the sensor and is closely followed by BK and then by ATP. The migration velocity of ATP varies more between CE runs than do the velocities of the other components, an observation consistent with the slower migration velocity of ATP (14). In separate studies, inhibitors to BK and ACh binding were used, and the results confirm the identifications presented in Fig. 3A.

Detection of components in complex biological matrices is a more challenging test of the power of this technique than the analysis of standard solutions. In Fig. 4, the CE-SCB fluorescence system identifies a species traditionally difficult to detect, ACh, which is present in the lysate of NGF-differentiated PC-12 cells (15). A sample containing an amount of material that corresponds to ~ 50 cells (16) was introduced into the separation capillary and electrophoretically separated while the fluorescence from a small group of PC-12 cells positioned near the capillary outlet was monitored. The resulting electropherogram (Fig. 4A) shows a single species that elicits a measurable change in $[Ca^{2+}]_i$ in the first 150 s of separation. This component, which migrates to the SCB detector in ~ 100 s, was identified as ACh by comparison with the electropherogram produced when an ACh standard solution was run (Fig. 4B).

A critical attribute for chemical sensors is an ability to detect minute quantities of material, and in this regard the CE-SCB fluorescence system compares favorably to the most sensitive analysis approaches. The lysate peak in Fig. 4A likely corresponds to a concentration of ACh in the low femtomole range (17), an amount approximately equal to the best detection limits for other methods (18). Of the species examined with the CE-SCB fluorescence system, the highest sensitivity is achieved for BK. To investigate the detection sensitivity and reproducibility for this species, we performed five CE runs of BK at each of three con-

J. B. Shear, H. A. Fishman, D. Garigan, R. N. Zare, Department of Chemistry, Stanford University, Stanford, CA 94305, USA.

N. L. Allbritton, Department of Neurobiology, Stanford University, Stanford, CA 94305, USA.

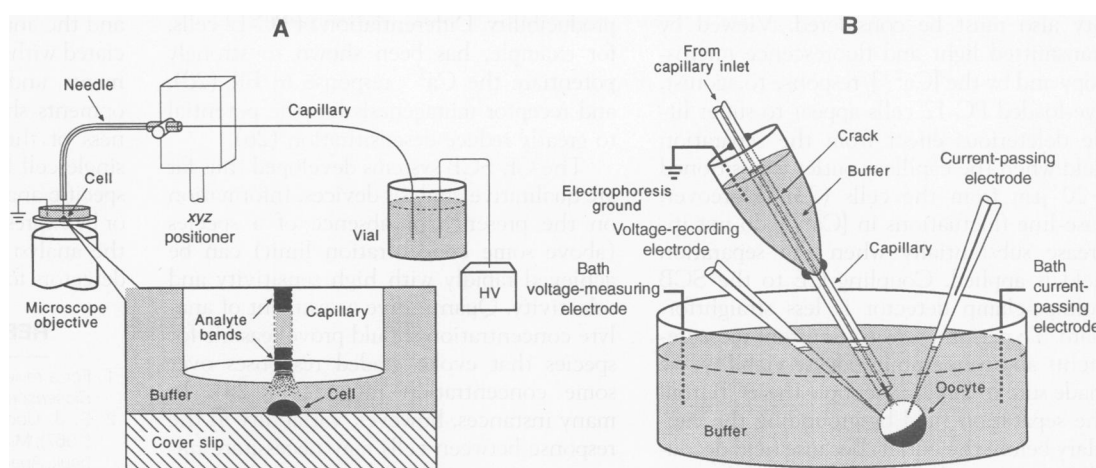
R. H. Scheller, Department of Molecular and Cellular Physiology, Stanford University, Stanford, CA 94305, USA.

*Present address: Applied and Engineering Physics Department, Cornell University, Ithaca, NY 14853, USA.

†Present address: Department of Physiology and Biophysics, University of California, Irvine, CA 92717, USA.

‡To whom correspondence should be addressed.

Fig. 1. Single-cell biosensor (SCB) systems for CE. **(A)** A CE-SCB device based on monitoring Ca^{2+} changes within one or more PC-12 cells with the use of the Ca^{2+} -sensitive dye fluo-3. Analytes were separated by capillary electrophoresis, and the capillary effluent was directed to PC-12 cells cultured on a microscope cover slip ~ 20 to $40 \mu\text{m}$ from the channel outlet. The capillary was threaded through a syringe needle and was glued at the needle entrance and exit points to stabilize the position of the outlet. Species that evoked changes in $[\text{Ca}^{2+}]_i$ were detected with an epi-illuminated fluorescence microscope. HV, high-voltage supply. **(B)** A CE-SCB system based on membrane current measurements on a *Xenopus laevis* oocyte expressing a cloned membrane receptor. Analytes that produced changes in the plasma membrane ion permeability after binding to the recep-



tor were detected with a two-electrode voltage-clamp amplifier. To reduce interferences from the separation field, the capillary was grounded upstream from the SCB through a narrow crack connecting the separation channel to a grounded electrolyte solution (24).

centrations with an individual cell as the sensor. A different PC-12 cell was selected as the SCB for each run, a step necessary to avoid detector desensitization (19), and care was taken to set the capillary outlet at the same distance ($40 \mu\text{m}$) from the cell for each run. At high ($10 \mu\text{M}$) and intermediate (100nM) concentrations, four of five and five of five cells, respectively, responded to BK after electrophoresis. At a low concentration (1nM), zero of five cells produced a clear response. These results indicate that the limit of detection is in the range of 1 to 100nM (~ 0.5 to 50amol), which is somewhat higher than reported values (20) for the minimum detectable BK concentration using the Ca^{2+} response of PC-12 cells (21). Nevertheless, the mass sensitivity of this system for BK is compet-

itive with fluorescence tagging and mass spectrometric analysis techniques (22), and a 10- to 100-fold improvement in sensitivity may be possible by differentiating the SCB (20).

The feasibility of tailoring a CE-SCB system to respond to specific components of interest is demonstrated in Fig. 5. A *Xenopus* oocyte microinjected with serotonin (5-hydroxytryptamine, or 5-HT) 5HT1c receptor mRNA was clamped at -70mV at the outlet of a separation capillary, and 5-HT was electrophoretically separated (Fig. 5A). No current response was seen for the blank (control) CE run (Fig. 5B), and the signal returned when 5-HT was separated once again (Fig. 5C). A slight increase in the migration time of 5-HT is apparent (Fig. 5, A and C), presumably caused by a decrease in the electroosmotic flow rate. A second control, in which the voltage-clamp measurement was made on an oocyte that is not microinjected with receptor mRNA, yielded no response for 5-HT after CE.

In coupling CE to an SCB, mechanical and electrical disturbances that may affect the detection sensitivity of the cell must be minimized. Small capillary movements can alter the relative position of the capillary and SCB, thereby changing the effective concentration of an analyte presented to the plasma membrane of an SCB. This effect can be dramatic when both the capillary i.d. and the cell diameter are small, as in the SCB fluorescence system. In addition, capillary movement may damage a cell and produce spurious detection signals when care is not taken to immobilize the column within the positioning needle. The effect of the separation field on cell integ-

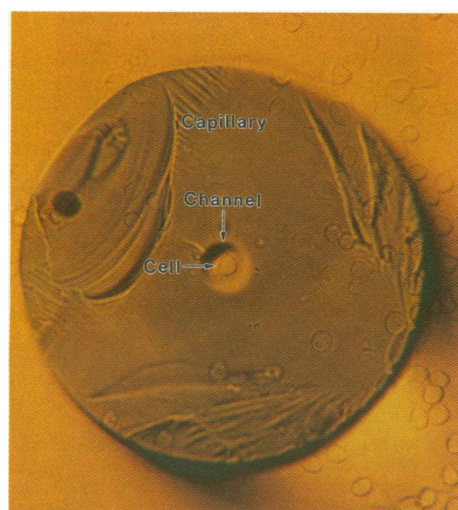
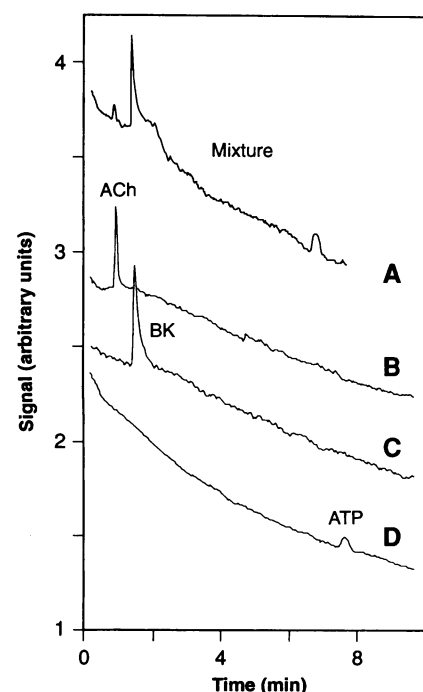


Fig. 2. A $25\text{-}\mu\text{m}$ i.d. capillary positioned above a single cell. For the CE-SCB fluorescence system, the capillary i.d. was 15 or $25 \mu\text{m}$, and 1 to 15 PC-12 cells were used as the analyte sensor.

Fig. 3. Identification of multiple components present in a mixture with the use of a CE-SCB system. **(A)** Separation of a mixture of ACh, BK, and ATP detected with the SCB fluorescence device. The three peaks in (A) were identified as ACh, BK, and ATP in **(B)**, **(C)**, and **(D)**, respectively, by electrophoretic separation of each component separately. Experimental conditions were as follows: 5-s gravity injections (inlet elevated 10 cm above outlet) of ACh (0.8mM), BK ($20 \mu\text{M}$), and ATP (5mM) were separated with an electric field of $\sim 850 \text{V/cm}$ in a $15\text{-}\mu\text{m}$ i.d. capillary. Between 10 and 15 PC-12 cells were used as the analyte sensor. The electropherograms are offset on the vertical axis to aid visualization. The negative baseline slope was caused by a decrease in the concentration of intracellular fluo-3; such a decrease can be compensated for by incorporation of fluo-3 AM ester in the measurement buffer.



Downloaded from www.sciencemag.org on June 29, 2013

riety also must be considered. Viewed by transmitted light and fluorescence microscopy and by the $[Ca^{2+}]_i$ response to agonist, dye-loaded PC-12 cells appear to suffer little deleterious effect from the separation field when the capillary outlet is positioned $\sim 20 \mu\text{m}$ from the cells (23). Moreover, base-line fluctuations in $[Ca^{2+}]_i$ do not increase substantially when the separation field is applied. Coupling CE to the SCB voltage-clamp detector is less straightforward. To perform sensitive current measurements and to maintain oocyte viability, we made sure to largely decouple the SCB from the separation field by grounding the capillary before the outlet. Because field decoupling is incomplete, application of the separation field increases baseline current fluctuations by approximately 10-fold (24).

The sensitivity and reproducibility of a CE-SCB system will vary markedly with analyte and cell type. Optimized detection limits for different ligands may range from more than picomoles to a few molecules (25). Factors that affect the detection signal include the ligand-receptor dissociation constant, the number of receptors exposed to ligand, the amplification pathways accessed after binding, the base-line variability in the quantity being measured, and frequently, the chemoreception history of the cell. Cellular response mechanisms can be manipulated to improve sensitivity and re-

producibility. Differentiation of PC-12 cells, for example, has been shown to strongly potentiate the Ca^{2+} response to BK (20), and receptor mutagenesis has the potential to greatly reduce desensitization (26).

The CE-SCB systems developed thus far are qualitative analysis devices. Information on the presence or absence of a species (above some concentration limit) can be achieved rapidly with high sensitivity and selectivity. Quantitative assessment of analyte concentration should prove feasible for species that evoke graded responses over some concentration range (27, 28). In many instances, however, variability in the response between cells may necessitate numerous separations to generate accurate dose-response relations. Alternatively, quantitation could be achieved by coupling the effluent from a CE capillary to a sensor comprised of many cells, although this approach may sacrifice mass sensitivity. Techniques for limiting cell-to-cell variability (29) and for reducing desensitization in re-used cells would aid in attempts to quantify analyte concentration.

Used qualitatively, the coupling of chemical separations with single-cell biosensors may prove valuable in a range of applications, including the isolation of novel ligands, the screening of mRNA expression,

and the analysis of very small volumes associated with single cells, subcellular compartments, and exocytosis. Quantitative developments should further expand the usefulness of this technique. The selectivity of single-cell biosensors can be engineered for specific analyses by transfection of cell lines or by expression of mRNA in oocytes, giving the analyst new power to rationally design detectors for biomolecular separations.

REFERENCES AND NOTES

1. For a review, see A. P. F. Turner, Ed., *Advances in Biosensors* (JAI Press, London, 1991).
2. S. J. Updike and G. P. Hicks, *Nature* **214**, 986 (1967); M. S. Abdel-Latif, A. A. Suleiman, G. G. Guibault, *Anal. Lett.* **21**, 943 (1988); I. Giaever, *J. Immunol.* **110**, 1424 (1973); N. Sugao, M. Sugawara, H. Minami, M. Uto, Y. Umezawa, *Anal. Chem.* **65**, 363 (1993); K. R. Rogers, J. J. Valdes, M. E. Eldefrawi, *Anal. Biochem.* **182**, 353 (1989).
3. J. W. Parce *et al.*, *Science* **246**, 243 (1989); H. Suzuki, E. Tamiya, I. Karube, *Anal. Chim. Acta* **199**, 85 (1987).
4. C. R. Gandhi, R. H. Behal, S. A. K. Harvey, T. A. Nouchi, M. S. Olson, *Biochem. J.* **287**, 897 (1992).
5. C. A. Monnig and R. T. Kennedy, *Anal. Chem.* **66**, 280R (1994).
6. T. M. Olefirowicz and A. G. Ewing, *ibid.* **62**, 1872 (1990); M. D. Oates, B. R. Cooper, J. W. Jorgenson, *ibid.*, p. 1573.
7. S. Nie, R. Dadoo, R. N. Zare, unpublished material.
8. J. R. Cooper, F. E. Bloom, R. H. Roth, *The Biochemical Basis of Neuropharmacology* (Oxford Univ. Press, New York, ed. 5, 1986), pp. 173-174; M. A. Rounds and S. S. Nielsen, *J. Chromatogr. A* **653**, 148 (1993).
9. Separations were performed in capillaries with an outer diameter of $360 \mu\text{m}$ and an inner diameter of 15, 25, or $40 \mu\text{m}$. Capillary lengths and separation fields ranged from 23 to 36 cm and 230 to 870 V/cm, respectively. The separation electrolyte buffer in all experiments matched the physiologic medium in which cells were maintained during measurement (10, 11).
10. Cells were cultured on a no. 1 cover slip and loaded with fluo-3 AM ester (Molecular Probes) at room temperature for ~ 0.5 hour. The loading medium contained 18 μM fluo-3, 135 mM NaCl, 5 mM KCl, 10 mM glucose, 2 mM $MgCl_2$, 2 mM $CaCl_2$, and 10 mM Hepes (pH 7.35). After loading, the cells were placed in the same medium without fluo-3 for 0.5 hour at room temperature. When cell recordings were made for long periods, 6 μM fluo-3 was often added to the medium to replenish the dye that was lost from the cells. The cells were transferred to the stage of a Diaphot-TMD-EF inverted fluorescence microscope (Nikon), where they were maintained at $\sim 35^\circ$ to 37°C by heating the $100\times$ (1.3 numerical aperture) oil-immersion lens used for illumination and fluorescence collection. Cells were illuminated with 470 to 490 nm light (Nikon filter block, B-1A), and fluorescence ($\lambda > 520 \text{ nm}$) was imaged onto an R928 photomultiplier tube (PMT) with a Microflex PFX photomicrographic attachment (Nikon). The current from the PMT was converted to a voltage and amplified with a LF355N operational amplifier. High-frequency noise was removed by a low-pass filter with a resistive-capacitive time constant of 1 s. The voltage signal was digitized by a DAS 8 analog-to-digital board (Metrabyte) and was displayed with customized software written in QuickBasic (Microsoft) on an AT personal computer (IBM).
11. Receptor complementary DNA was transcribed in vitro to yield mRNA at a concentration of $\sim 0.1 \mu\text{g}/\mu\text{l}$. Stage V and VI *Xenopus* oocytes were microinjected with 50 nl of mRNA per cell, and oocytes were incubated in ND96 solution [96 mM NaCl, 2 mM KCl, 1.8 mM $CaCl_2$, 1 mM $MgCl_2$, 5 mM Hepes at pH 7.2, 2.5 mM sodium pyruvate, penicillin (100 U/ml), and streptomycin (100 $\mu\text{g}/\text{ml}$)], for ~ 24 hours at 18°C . Before microinjection, the follicular cell layer was re-

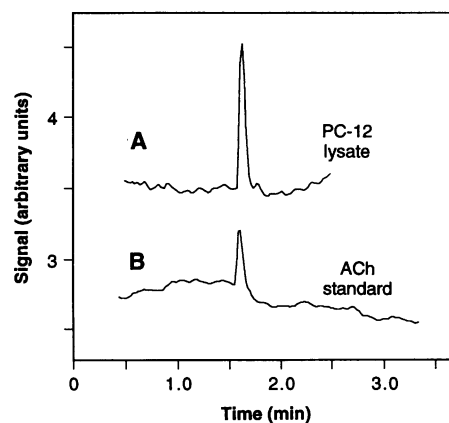


Fig. 4. Identification of a single component present in a complex biological matrix with the use of the CE-SCB fluorescence system. In (A), a sample derived from the lysate of PC-12 cells was electrophoretically separated, producing a single peak in the first 150 s of separation. This peak was identified as ACh in (B) by electrophoretic separation of a standard solution and comparison of the migration times of the unknown and the standard. Experimental conditions were as follows: 10-s gravity injections (+10 cm above the outlet) of lysate and ACh standard (0.8 mM) were separated with a field of $\sim 400 \text{ V/cm}$ in a $25\text{-}\mu\text{m}$ i.d. capillary. Between four and five PC-12 cells were used as the sensor. The electropherograms are offset on the vertical axis. Fluo-3 AM ester was included in the measurement buffer.

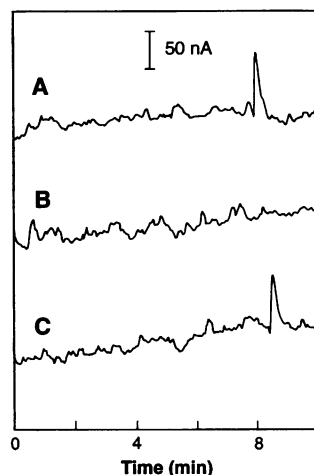


Fig. 5. Electropherograms demonstrating the feasibility of tailoring a CE-SCB system to respond to specific components. A *Xenopus* oocyte expressing the cloned rat 5HT1c receptor was clamped at -70 mV , and the current flow across the plasma membrane was monitored during electrophoresis. In (A), a sample containing serotonin (5-HT) was injected into the capillary and was electrophoretically separated, producing a peak at ~ 8 min. The electropherogram in (B) demonstrates that no response was obtained when a blank sample was run, and (C) shows the return of the peak when 5-HT was once again separated. Experimental conditions were as follows: 20-s gravity injections (+13 cm above the outlet) of 5-HT (100 μM) or blank buffer solution were separated at $\sim 250 \text{ V/cm}$ in a $40\text{-}\mu\text{m}$ i.d. capillary.

- moved from the oocyte by digestion with collagenase (2 mg/ml, type IA, Sigma). Two-electrode voltage-clamp measurements were performed with a TEV-200 amplifier (Dagan) in the virtual-current mode. Intracellular Ag-AgCl electrodes were constructed with an initial input impedance of ~3 to 4 megohms through 3 M KCl single-pull pipettes. The oocyte bath solution for measurements contained 140 mM NaCl, 2 mM KCl, 2 mM CaCl₂, and 10 mM Hepes (pH 7.2).
12. A narrow crack connecting the capillary channel to a grounded electrolyte reservoir was made ~10 cm upstream from the capillary outlet with the technique described in M. C. Linhares and P. T. Kissinger [*Anal. Chem.* **63**, 2076 (1991)].
 13. T. Pozzan, F. DiVirgilio, L. M. Vicentini, J. Meldolesi, *Biochem. J.* **234**, 547 (1986); S. B. Sands and M. E. Barish, *Brain Res.* **560**, 38 (1991); C. Fasolato, P. Pizzo, T. Pozzan, *J. Biol. Chem.* **265**, 20351 (1990).
 14. Divalent cations in the separation buffer interacted with the capillary surface, causing a slow decrease in the electroosmotic flow rate until equilibrium was reached [see K. Yamamoto, S. Suzuki, M. Ueda, K. Takehi, *J. Chromatogr.* **588**, 327 (1991)]. This decrease reduced the velocity of a slow species by a greater relative amount than the velocity of a fast species (assuming migration velocities remain positive).
 15. A 50-ml culture flask of PC-12 cells differentiated for 4 days in medium containing β -NGF (25 ng/ml) was pelleted, and cells were lysed in ~70 μ l of 70% methanol containing ~0.1 mM eserine to inhibit cholinesterase activity.
 16. With the use of the Hagen-Poiseuille equation and estimations of diffusion and spontaneous fluid displacement [see H. A. Fishman *et al.*, *Anal. Chem.* **66**, 2318 (1994)], the injection volume was calculated to be ~500 pl. This volume corresponds to ~10⁻⁵ of the entire lysate volume. Cells were differentiated at ~10% confluence (that is, ~5 \times 10⁶ cells were incorporated into the lysate), so that the sample volume contained the equivalent of ~50 cells.
 17. L. A. Greene and G. Rein, *Nature* **268**, 349 (1977).
 18. M. D. Greaney, D. L. Marshall, B. A. Bailey, I. N. Acworth, *J. Chromatogr. Biomed. Appl.* **622**, 125 (1993).
 19. The Ca²⁺ response to BK was observed to decrease substantially when multiple CE runs were performed in a short period.
 20. A. B. Bush, L. A. Borden, L. A. Greene, F. R. Maxfield, *J. Neurochem.* **57**, 562 (1991).
 21. This result may be caused by sample dilution in the capillary-SCB transfer region.
 22. T. B. L. Kist, C. Termignoni, H. P. H. Grieneisen, *Braz. J. Med. Biol. Res.* **27**, 11 (1994); R. D. Smith, J. H. Wahl, D. R. Goodlett, S. A. Hofstadler, *Anal. Chem.* **65**, 574A (1993).
 23. At gap distances less than 20 μ m, damage was sometimes apparent. Electrical and mechanical distress both may contribute to cell damage when very small gap distances are used.
 24. "Grounding" through a crack in the capillary creates a voltage splitter, in which the relative current through the crack and to the end of the capillary is determined by the relative resistances of the two paths. Although most of the current passes through the crack, some residual current flows through the capillary outlet and interferes with the voltage-clamp measurement.
 25. M. Mori *et al.*, *J. Biol. Chem.* **263**, 14574 (1988).
 26. T. Jackson, *Pharmacol. Ther.* **50**, 425 (1991).
 27. C. A. Briggs *et al.*, *Br. J. Pharmacol.* **104**, 1038 (1991).
 28. E. M. DeLorme and R. McGee Jr., *J. Neurochem.* **50**, 1248 (1988).
 29. L. A. Greene, M. M. Sobehi, K. K. Teng, in *Culturing Nerve Cells*, G. Banker and K. Goslin, Eds. (MIT Press, Cambridge, MA, 1991), pp. 207-226.
 30. We thank L. Stryer and R. Dadoo for stimulating discussions, and Z.-J. Xu, S.-C. Hsu, C. Sims, and R. Schneevis for technical assistance. We gratefully acknowledge the laboratories of E. Shooter and D. Julius for the donation of PC-12 cells and 5HT1c complementary DNA, respectively. J.B.S. is a Howard Hughes Predoctoral Fellow, and H.A.F. is a W. R. Grace Fellow. Supported by grants from the National Institute of Mental Health (MH45423-03 and MH45324-05) and Beckman Instruments.

2 September 1994; accepted 1 November 1994

Permian-Triassic Life Crisis on Land

G. J. Retallack

Recent advances in radiometric dating and isotopic stratigraphy have resulted in a different placement of the Permian-Triassic boundary within the sedimentary sequence of the Sydney Basin of southeastern Australia. This boundary at 251 million years ago was a time of abrupt decline in both diversity and provincialism of floras in southeastern Australia and extinction of the *Glossopteris* flora. Early Triassic vegetation was low in diversity and dominated by lycopods and voltzialean conifers. The seed fern *Dicroidium* appeared in the wake of Permian-Triassic boundary floral reorganization, but floras dominated by *Dicroidium* did not attain Permian levels of diversity and provinciality until the Middle Triassic (244 million years ago).

The Permian-Triassic boundary has long been known as a major discontinuity in the history of life in the sea (1), but comparably severe extinctions have not been apparent from recent assessments of the fossil record of land plants (2) or animals (3). Geochemical approaches to the vexing problem of correlation between marine and nonmarine biostratigraphic schemes give grounds

for reassessing Permian-Triassic boundary events on land. High-precision ²⁰⁶Pb/²³⁸U radiometric dating of zircons from a tuff at the Permian-Triassic boundary in marine sequences of China at 251 ± 3.4 (2 σ) million years ago (Ma) (4), supported by dating of tuffs in coal measures of the Gunnedah and Sydney basins of New South Wales (5), now indicates that the Permian-Triassic boundary is near the contact between coal measures with *Glossopteris* and overlying fluvial deposits with *Dicroidium*

throughout the Bowen-Gunnedah-Sydney basins of eastern Australia. Ironically, this was the traditionally recognized Permian-Triassic boundary in Australia until 1970 (6). At that time, correlation of palynomorph assemblages from Australia with those of Pakistan encouraged the view that the boundary was significantly higher in the sequence: at the top of the palynozone characterized by *Protohaploxypinus microcorpus* (7). Recent chemostratigraphic studies of boreholes in the Canning Basin of Western Australia have demonstrated that ¹³C/¹²C ratios in kerogen of marine shale became abruptly lower at the Permian-Triassic boundary (8). This dramatic isotopic excursion is characteristic of numerous marine sections through the Permian-Triassic boundary (9) and has been recognized also within nonmarine sequences of the Cooper, Bowen, and Sydney basins at the base of the *P. microcorpus* palynozone (10).

The transition from *Glossopteris* to *Dicroidium* floras is abrupt and profound. Only four genera and one species of megafossil plants are known to have survived the boundary in the Sydney Basin (11), an extinction of 97% of Late Permian fossil leaf species. Leaves of *Glossopteris* have been found in claystone partings of the uppermost (or Bulli) coal only 19 cm below shales bearing *Dicroidium callipteroides* (12). I restricted my analysis to fossil leaves (Fig. 1) to avoid duplication of names for fructifications (13), but the Permian-Triassic crisis also curtailed the Late Permian evolutionary adaptive radiation of glossopterid fructifications in Gondwana (14).

Fossil plants replacing the *Glossopteris* flora were low in diversity (Fig. 1). Although the zonal indicator is the distinctive seed fern *D. callipteroides*, many assemblages are dominated by the conifer *Voltziopsis* (15) or the lycopod *Cylomeia* (16). These voltzialean conifers and small Isoetes-like lycopods are most closely allied to Eurasian Early Triassic genera such as *Annalepis*, *Tomiostrabus*, and *Voltzia* (17). Both *Voltziopsis* and *Cylomeia* persist into diverse later floras dominated by the Gondwanan endemic seed fern, *Dicroidium zuberi*. Diversification of Gondwanan seed ferns continued with the appearance in the Middle Triassic of *Dicroidium odontopteroides*, a biostratigraphic event that has been dated in New Zealand at about 244 Ma (18). The seed fern *D. odontopteroides* is a prominent element of diverse fossil floras that show regional differentiation throughout southern Pangaea (19). In Eurasia similarly, extinction of ruflorian and voynovskyan cordaites was followed by an interregnum of conifers and lycopods, which were supplanted by diverse Middle Triassic floras dominated by the seed fern *Scytophyllum* (17).

The megafossil plant record of Permian-

Department of Geological Sciences, University of Oregon, Eugene, OR 97403-1272, USA.